1986ApJ...311..197A

THE ASTROPHYSICAL JOURNAL, 311:197–213, 1986 December 1
© 1986. The American Astronomical Society. All rights reserved. Printed in U.S.A.

VORTEX CREEP AND THE INTERNAL TEMPERATURE OF NEUTRON STARS: TIMING NOISE IN PULSARS

M. ALI ALPAR
Scientific and Technical Research Council of Turkey, Research Institute for Basic Sciences

RADHA NANDKUMAR
National Center for Supercomputing Applications, University of Illinois, Champaign

AND

DAVID PINES
Department of Physics, University of Illinois, Urbana
Received 1986 February 28; accepted 1986 May 9

ABSTRACT

Vortex creep theory is used to construct model noise power spectra for three physically distinct types of events which might give rise to pulsar timing noise: events which are a consequence of vortex unpinning, events which involve vortex unpinning along with some physical process in the pinning region other than vortex unpinning, and "external" events in which the initial frequency jumps responsible for noise do not involve any vortex unpinning. It is shown that for the first two types of events, relaxation processes in the pinning region give rise to structure in the observed power spectra, while for external events, noise power spectra are not significantly influenced by vortex creep. Our theoretical results are compared with the analysis by Boynton and Deeter of the power spectra of 25 pulsars. The absence of structure in the observed power spectra of the Crab and Vela pulsars within the range of time scales which characterize their postglitch behavior indicates that the pinning regions which play a role in postglitch behavior do not experience the small unpinning events leading to timing noise. This may, mean that one has a threshold for glitches produced by vortex unpinning, a threshold sufficiently large that vortex unpinning plays no observable role in the timing noise of these pulsars. For the remaining pulsars, our search for structure is carried out by using the observational data to construct rejection contours in the (Q^{-1}, log τ)-plane; here Q is the fraction of a frequency jump which subsequently relaxes with a characteristic time τ. There is at present no clear evidence of structure, but for many pulsars there remains a substantial region of (Q, τ)-parameter space which is not yet explored. Our present results are consistent with the hypothesis that physical processes in regions external to the weak and superweak pinning regions so far explored in postglitch observations are responsible for the timing noise in pulsars; however, further observations will be required to place this conclusion on a firm footing.

Subject headings: pulsars — stars: neutron

I. INTRODUCTION

The observed pulsation periods of pulsing X-ray sources and pulsars are interpreted as the rotational periods of the neutron star crust. Any fluctuation in this period, exhibited as timing noise, is indicative of a fluctuation in the rotation rate of the crust. This could arise from either external or internal torque variations. The external accretion torque noise is expected to dominate the timing noise from accreting binary X-ray sources (Lamb 1985), while internal torque variations represent a possible cause of timing noise in pulsars. Timing noise in the Crab pulsar was first studied by Boynton *et al.* (1972) and later by Groth (1975). Their analysis indicates that superposed on the smooth spin-down behavior, which is describable in terms of a low-degree polynomial, is a random fluctuation in pulse phase. This random component is in the form of a random walk in the rotation frequency for the Crab pulsar. A similar analysis by Cordes (1980) and Cordes and Helfand (1980) of the timing behavior of 50 pulsars establishes that timing noise is a general characteristic of many pulsars. A detailed analysis of 11 of the pulsars in that sample (Cordes and Helfand 1980) indicates that two pulsars show a random walk in rotation phase, two show a random walk in rotational acceleration, and the remaining candidates show a random walk in frequency.

Lamb, Pines, and Shaham (1978*a*, *b*) have developed a theoretical description, based on noise processes, of torque fluctuations responsible for the period variations. They have analyzed the response of a two-component star to such torque fluctuations and show how such a description can be used to determine both the properties of the torque fluctuations and the internal structure of neutron stars. One particularly interesting application of their theory has been the use of timing noise data to place limits on the two-component model of neutron star structure (Boynton 1981). Cordes and Downs (1985) have analyzed the JPL data for some two dozen pulsars and have subjected long data stretches to a variety of tests to determine the statistical nature of timing activity. They find that for many pulsars simple random-walk processes comprising solely step functions in the phase or one of its derivatives are not consistent with the data, and that the processes have events in which steps in both the frequency and its derivative take place. An alternative approach to analyzing pulsar timing data, based on a systematic methodology for estimation of red power spectra, has been developed by Deeter and Boynton (1982). In Boynton and Deeter (1985) they use it to analyze the noise spectra of the JPL data for the same pulsars considered by Cordes and Downs; their representation, which leads to results which are

© American Astronomical Society • Provided by the NASA Astrophysics Data System

1986ApJ...311..197A

consistent with those of Cordes and Downs, is particularly convenient for comparison with the theoretical models we consider below.

Timing noise analysis is also of great interest in view of the unprecedented stability of the millisecond pulsar PSR 1937+21. Recently Blandford, Narayan, and Romani (1984) have carried out a noise analysis for the millisecond pulsar to estimate the sensitivity of fast pulsars as detectors of gravitational radiation and to find limits on the use of accurate arrival times to measure pulsar spin-down, position, proper motion, and distance, in the presence of a particular noise spectrum.

The present paper is devoted to an examination of the possible role of internal torque fluctuations in pulsar timing noise. The success of vortex creep theory (Alpar *et al.* 1984*a*) in explaining the postglitch behavior of the Vela pulsar PSR 0833−45 (Alpar *et al.* 1984*b*), the Crab pulsar PSR 0531+21, and PSR 0525+21 (Alpar, Nandkumar, and Pines 1985) indicates that in these pulsars large-scale glitch behavior is dominated by the behavior of vortices in the crustal neutron superfluid. The pinning and unpinning of the superfluid vortices to the crustal nuclei gives rise to substantial internal torque variations. It seems natural, therefore, to explore whether small-scale internal torque fluctuations produced by the pinned crustal superfluid can be responsible for the observed timing noise.

We begin investigating the contribution of vortex creep torque fluctuations to timing noise. As we shall see, vortex creep (the thermal motion of pinned vortices) depends exponentially on the departure $\delta\omega$ of the frequency lag $\omega = \Omega - \Omega_c$ from its steady state value; here Ω is the rotational frequency of the pinned superfluid and Ω_c is that of the stellar crust. Whenever there is a change in either Ω or Ω_c, the vortex creep process is altered. Hence, the fluctuations in the internal torque could be due to randomly occurring vortex unpinning events that change the superfluid rotation rate and the subsequent response of vortex creep; an alternative possibility is that processes external to the pinned superfluid affect the crustal angular velocity and evoke a vortex creep response. If the angular momentum transfer to the crust in such events is small enough so that individual events are not resolved, then a simple noise description is appropriate.

In § II we review vortex creep theory and use it to construct model noise power spectra. In § III we compare these spectra with observations; § IV contains our conclusions.

II. VORTEX CREEP THEORY AND NOISE MODELS

An event characterized by a sudden jump $\Delta\Omega_c$ in the crustal frequency will be accompanied by a change in the spin-down rate of the form

$$\Delta\dot{\Omega}_c(t) = \Delta\Omega_c\,\delta(t) + \Delta\dot{\Omega}_{c,r}(t)\,, \tag{2.1}$$

where $\Delta\dot{\Omega}_{c,r}(t)$ is the response of the internal torques to the frequency jump $\Delta\Omega_c$. This description is equally applicable to large-scale glitches and to small-scale events which cannot be resolved and make up the noise process.

In vortex creep theory, the internal torque produced in response to a glitch by the crustal neutron superfluid in a given pinning layer takes the form

$$N_{\rm int}{}^i(t) = I_i|\dot{\Omega}_\infty|\,\frac{1}{1+(e^{t_{0i}/\tau_i}-1)e^{-t/\tau_i}}\,, \tag{2.2}$$

where I_i is the inertial moment of the layers and τ_i is the relaxation time which describes its approach to steady state (Alpar *et al.* 1984*a*),

$$\tau_i = \left(\frac{\omega_{\rm cr}}{E_p}\right)_i \frac{k_B T}{|\dot{\Omega}_\infty|}\,. \tag{2.3}$$

Here $(\omega_{\rm cr})_i$ is the maximum lag which can be supported by the pinning force, and $(E_p)_i$ is the pinning energy associated with region i. The postglitch delay time t_{0i} is determined by the glitch-induced change in the angular velocity profile $\delta\omega_i$,

$$t_{0i} = \delta\omega_i(t=0^+)/|\dot{\Omega}_\infty|\;; \tag{2.4}$$

$\Delta\dot{\Omega}_{c,r}{}^i$ is given by the change in the internal torque produced by the event,

$$\Delta\dot{\Omega}_{c,r}{}^i(t) = \frac{N_{\rm int}{}^i(t)}{I_c} - \frac{N_{\rm int}{}^i(0^-)}{I_c}\;; \tag{2.5}$$

if we assume that the pinned vortices were in a steady state prior to the event, then $N_{\rm int}(0^-) = I_i|\dot{\Omega}_\infty|$, which yields

$$\Delta\dot{\Omega}_{c,r}{}^i(t) = \frac{I_i|\dot{\Omega}_\infty|}{I_c}\,\frac{[e^{t_{0i}/\tau_i}-1]e^{-t/\tau_i}}{1+[e^{t_{0i}/\tau_i}-1]e^{-t/\tau_i}}\;; \tag{2.6}$$

I_c is the moment of inertia of the crust and all components of the star that are coupled rigidly to the crust. On time scales longer than minutes, this includes the core superfluid, so that I_c is practically the total moment of inertia of the star for our purposes (Alpar, Langer, and Sauls 1984).

We use equation (2.2) to calculate the response of the vortex creep torque to three physically distinct types of events: (1) the initial frequency jump is a consequence of vortex unpinning, (2) the initial frequency jump is produced by some physical process other than vortex unpinning but leads to the unpinning of some vortices, and (3) the event does not involve any vortex unpinning. In each case we compute the expected power spectrum for a constant representative value of τ. We then consider to what extent the observed timing noise from pulsars can be interpreted in terms of these physically distinct types of events.

a) Pure Unpinning Events

We model the noise process as a series of events, each of which is a scaled down version of a pulsar glitch; in each event the moment of inertia of the regions through which the unpinned vortices move is very much smaller than the total moment of inertia of the pinned superfluid. Thus the number of vortices N that unpin is much smaller than those which unpin in a typical glitch, and these vortices recouple within a short distance. We assume that N vortices of uniform density δn_G in a region G of width δr_G suddenly unpin, move outward through a region B, and repin in a region G', as shown in Figure 1*a*. The vortex density distribution through these regions G and G' is related to the number of vortices N by

$$2\pi r\delta r_G|\delta n_G| = 2\pi r\delta r_{G'}|\delta n_{G'}| = N \tag{2.7}$$

and to the change in superfluid angular velocity in the region B by

$$\delta\Omega_B = N\kappa/2\pi r^2\,. \tag{2.8}$$

For uniform δn_G and $\delta n_{G'}$, the superfluid angular velocity changes linearly in the regions G and G'; the profile of the change in superfluid angular velocity is shown in Figure 1*b*. Here, $\kappa = h/2m_n$ is the quantum of vorticity, 2×10^{-3} cm^2 s^{-1};

© American Astronomical Society • Provided by the NASA Astrophysics Data System

1986ApJ...311..197A

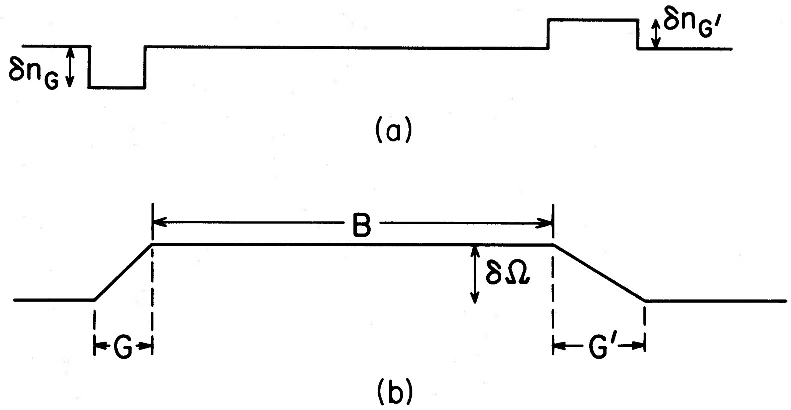

FIG. 1.—Change in vortex density δn resulting from the unpinning of N vortices in region G which then repin in region G'. (b) Resulting change $\delta\Omega$ in the superfluid rotation rate.

and r, the distance from the rotation axis, is approximately the stellar radius.

Such an event leads to an angular momentum transfer to the crust of magnitude

$$\Delta L = I_c\, \Delta\Omega_{c,u} = (I_A/2 + I_B)\delta\Omega_B \;, \tag{2.9}$$

where I_G, $I_{G'}$, I_B, and I_c are the moments of inertia of the regions G, G', B, and the crust respectively; $I_A = I_G + I_{G'}$; and $\Delta\Omega_{c,u}$ is the jump in the rotation frequency of the crust due to unpinning. If I_A and I_B are much smaller than $I_p \approx 10^{-2} I_c$, then

$$\Delta\Omega_{c,u} \ll 10^{-2}\delta\Omega_B \;. \tag{2.10}$$

The change in the lag $\omega = \Omega - \Omega_c$ is defined by $\delta\omega = \Delta\Omega_c + \delta\Omega$. In the regions of the pinned superfluid through which no vortex motion has occurred, $\delta\omega$ is determined solely by $\Delta\Omega_{c,u}$, while $\delta\omega$ is determined by $\delta\Omega$ in the regions G, G', and B through which unpinned vortices have moved. Thus, on making use of equation (2.10), we find

$$\delta\omega = \Delta\Omega_{c,u}, \quad \text{everywhere outside } G, G'; \text{ and } B \;, \tag{2.11a}$$

$$\begin{aligned} \delta\omega &= \delta\Omega_B(r - a_1)/\delta r_G + \Delta\Omega_{c,u} \\ &\approx \delta\Omega_B(r - a_1)/\delta r_G, \quad \text{in region } G \;, \end{aligned} \tag{2.11b}$$

$$\begin{aligned} \delta\omega &= \delta\Omega_B + \Delta\Omega_{c,u} \\ &\approx \delta\Omega_B \;, \quad \text{in region } B \;, \end{aligned} \tag{2.11c}$$

$$\begin{aligned} \delta\omega &= \delta\Omega_B(a_2 - r)/\delta r_{G'} + \Delta\Omega_{c,u} \\ &\approx \delta\Omega_B(a_2 - r)/\delta r_{G'} \;, \quad \text{in region } G' \;. \end{aligned} \tag{2.11d}$$

Equation (2.6) gives the response of the vortex creep torque to the change in lag given by equation (2.11c). The response to the changes in lag given by equations (2.11b) and (2.11d) is obtained by integrating $\Delta\dot{\Omega}_{c,r}(t)$ in equation (2.6) over the regions G and G'; it is

$$\begin{aligned} \Delta\dot{\Omega}_{c,r}(t > 0^+) = &-\frac{I_B|\dot{\Omega}_\infty|\theta(t)}{I_c}\,\frac{[e^{-t/\tau}(e^{t_0/\tau} - 1)]}{[1 + e^{-t/\tau}(e^{t_0/\tau} - 1)]} \\ &-\frac{I_A|\dot{\Omega}_\infty|}{I_c}\,\theta(t)\left\{1 - \frac{1 - \tau/t_0 \ln\left[1 + (e^{t_0/\tau} - 1)e^{-t/\tau}\right]}{1 - e^{-t/\tau}}\right\}, \end{aligned} \tag{2.12}$$

where $t_0 = \delta\Omega_B/|\dot{\Omega}_\infty|$ and $I_A = I_G + I_{G'}$. The complete event (unpinning and response) is

$$\Delta\dot{\Omega}_c(t) = \Delta\Omega_{c,u}\delta(t) + \Delta\dot{\Omega}_{c,r}(t) \;, \tag{2.13}$$

where $\Delta\Omega_{c,u}$ as given by equation (2.9) is related to the coefficients of $\Delta\Omega_{c,r}$. Note that the mean change in $\dot{\Omega}_c$ vanishes,

$$\int_{0^-}^{\infty} \Delta\dot{\Omega}_c(t)dt = 0 \;, \tag{2.14}$$

and, from equation (2.14),

$$\lim_{T\to\infty} \{\Delta\Omega_c(T) - \Delta\Omega_c(0^-)\} = 0; \tag{2.15}$$

the jump in the crustal frequency relaxes back completely. Quite generally, one can introduce a parameter Q to characterize the fraction of the frequency jump which subsequently relaxes, as was previously done in the two-component model of Baym *et al.* (1969):

$$Q \equiv \frac{\int_{0^+}^{\infty} \Delta\dot{\Omega}_{c,r}(t)dt}{\Delta\Omega_{c,u}} \;. \tag{2.16}$$

From equation (2.14) we see that a pure unpinning event has $Q = 1$.

When $t_0 \ll \tau$, the timescale for the perturbation is small compared to the underlying time scale τ of the creep process, and the response follows the initial unpinning event with an exponential relaxation of time constant τ; thus

$$\Delta\dot{\Omega}_{c,r}(t) = -\frac{[(I_A/2) + I_B]}{I_C}\,\frac{\delta\Omega_B e^{-t/\tau}\theta(t)}{\tau}\;(t_0 \ll \tau) \;. \tag{2.17}$$

When $t_0 \gg \tau$, the large extent of unpinning alters the vortex creep in the regions G, G', and B:

$$\Delta\dot{\Omega}_{c,r}(t) = \frac{[I_A(1 - t/t_0) + I_B]|\dot{\Omega}_\infty|\{\theta(t) - \theta(t - t_0)\}}{I_C} \times (t_0 > t \gg \tau) \;. \tag{2.18}$$

The response of region B is nearly zero at $t = 0$; it begins to be appreciable around $t \approx t_0$; the assumed linear variation in $\delta\Omega$ in regions G and G' leads to a gradual recoupling linear in t in these regions.

We assume that the noise process consists of individual unpinning events followed by vortex creep response. We also assume that the unpinnings occur at random times t_i and at a rate R such that during an interval T, the number of events obeys a Poisson distribution with a mean value RT, and the times t_i are uniformly distributed for $0 < t_i < T$. The residual

© American Astronomical Society • Provided by the NASA Astrophysics Data System

1986ApJ...311..197A

in $\dot{\Omega}_c(t)$, after removal of an apppropriate polynomial contribution, can be written as

$$\delta\dot{\Omega}_c(t) = \sum_i \Delta\dot{\Omega}_c(t - t_i) \tag{2.19}$$

and has the form of shot noise (Lamb, Pines, and Shaham, 1978*a*, *b*). Here shot noise denotes random occurrences of pulses of a particular shape. For simplicity, we assume that all events have the same value of the parameters I_A, I_B, t_B, and τ. The results can be generalized easily by replacing these parameters with the appropriate moments of their distributions. For shot noise, we define

$$S(\omega) = \int_{-\infty}^{\infty} \Delta\dot{\Omega}_c(t) \exp(i\omega t)dt \ ; \tag{2.20}$$

the power spectrum of the noise in the variable $\dot{\Omega}$, $P_{\dot{\Omega}}(f)$, where $f = (\omega/2\pi)$, is then

$$P_{\dot{\Omega}}(f) = R\,|S(\omega)|^2 \ , \tag{2.21}$$

following the treatment in Rice (1954). For infinite data stretches, i.e., $T \to \infty$, f is a continuous variable; for T finite, the power given by equation (2.21) resides at discrete frequencies $f = n/T$, where n is an integer, For $\Delta\dot{\Omega}_c(t)$ given by equation (2.13), for any given t_0 and τ we get

$$S(\omega) = \left[\frac{(I_A/2 + I_B)}{I_C}\right]\delta\Omega_B - \left(\frac{I_B}{I_C}\right)|\dot{\Omega}_\infty|\tau \times \sum_{k=1}^{\infty} A'^k B(1 + i\omega\tau; k) - \frac{(I_A/I_C)}{i\omega t_0}|\dot{\Omega}_\infty|\tau \times \sum_{k=1}^{\infty} \frac{A'^{k+1}}{k+1}[1 - kB(1 + i\omega\tau; k)] \ , \tag{2.22}$$

where

$$A' = (1 - e^{-t_0/\tau}) \ , \tag{2.23}$$

$$B(a; b) = \Gamma(a)\Gamma(b)/\Gamma(a + b) \ , \tag{2.24}$$

and $\Gamma(a)$ is the gamma function.

The noise spectrum takes a simple form in a number of cases of physical interest. Thus, one finds readily that for the limiting case of $t_0 \ll \tau$,

$$S(\omega) = \Delta\Omega_{c,u}\, i\omega\tau/(1 + i\omega\tau) \ , \tag{2.25}$$

$$P_{\dot{\Omega}}(f) = R(\Delta\Omega_{c,u})^2\omega^2\tau^2/(1 + \omega^2\tau^2) \ , \tag{2.26}$$

while for $t_0 \gg \tau$, and $\omega t_0 \ll 1$,

$$S(\omega) = [(I_A/6 + I_B/2)/I_C]\delta\Omega_B\, i\omega t_0 \ , \tag{2.27}$$

$$P_{\dot{\Omega}}(f) = R[(I_A/6 + I_B/2)/I_C]\delta\Omega_B{}^2\omega^2 t_0{}^2 \ , \tag{2.28}$$

and when $t_0 \gg \tau$ and $\omega t_0 \gg 1$,

$$S(\omega) = \Delta\Omega_{c,u} \ , \tag{2.29}$$

$$P_{\dot{\Omega}}(f) = R(\Delta\Omega_{c,u})^2 \ . \tag{2.30}$$

The nature of these power spectra is easy to understand. When ω is small, autocorrelation times are long compared to the time scale of the response (which is the larger of t_0 and τ), and each event is fully sampled; the event in $\dot{\Omega}$ is the derivative of a δ-function, and the corresponding event in Ω is a δ-function. Hence, the noise in Ω appears white; $P_\Omega(f)$ is independent of frequency, and $P_{\dot{\Omega}}(f)$ is proportional to ω^2 for both $t_0 \ll \tau$ (eq. [2.26] in the limit $\omega\tau \ll 1$) and for $t_0 \gg \tau$ (eq. [2.28]).

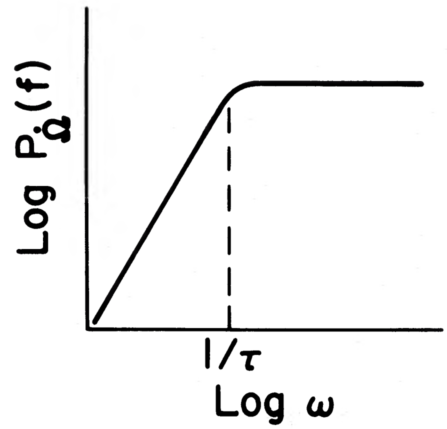

FIG. 2.—Logarithm of power density for a pure unpinning noise vs. logarithm of frequency. At $\omega \approx 1/\tau$, the spectrum changes from a slope 2 to slope 0.

For large ω, however, there is only a contribution from the unpinning part of the event, since the response time scales τ or t_0 only contain frequencies ω less than τ^{-1} or $t_0{}^{-1}$. Therefore, for large ω, the $\dot{\Omega}$ events consist of a series of δ-functions, and hence $P_{\dot{\Omega}}(f) = \text{constant}$; one finds white noise in $\dot{\Omega}$ for $\omega \gg \tau^{-1}$ (eq. [2.26] in the limit $\omega\tau \gg 1$ and eq. [2.30]).

Note the characteristic shoulder in the power spectrum at frequencies $f \approx 1/2\pi\tau$ or $1/2\pi t_0$. Such a shoulder will emerge in an observational power spectrum if the range of autocorrelation times spanned by the data includes either the relaxation time τ, if $\tau \gg t_0$, or the offset time t_0, if $t_0 \gg \tau$. A plot of log $P_{\dot{\Omega}}(f)$ versus log ω is given in Figure 2.

b) Mixed Events

When the initial frequency jump is initiated by physical processes other than vortex unpinning but leads to vortex unpinning, we denote the resulting events as "mixed events." Such events could result, for example, from breaking of the inner crust lattice by pinned vortex lines, as proposed by Ruderman (1976) to explain giant glitches. Although the lattice may be too strong to make this a likely mechanism for glitches, local variations in the vortex density and pinning force involving a small pocket of vortex lines could provide enough local stress to break the lattice and so give rise to unpinning and outward motion of the vortex lines. Pinned vortices exert a radial stress on the lattice; thus the moment of inertia of the lattice would change by a small amount δI, giving rise to a change in Ω_c; by contrast, unpinning leads to an increase $\Delta\Omega_{c,u}$. The effective change in Ω_c can be written as

$$\Delta\Omega_c/\Omega_c = (\Delta\Omega_{c,u}/\Omega_c) - (\delta I/I_c) \equiv Q^{-1}\Delta\Omega_{c,u}/\Omega_c \ , \tag{2.31}$$

where Q, as given by equation (2.16), characterizes the extent to which vortex unpinning plays a role in the event; as we have seen, $Q = 1$ corresponds to pure unpinning. A particularly interesting case is $Q \gg 1$, that is $|\Delta\Omega_c| \ll \Delta\Omega_{c,u}$. Using the simple model of § II*a* for the regions through which vortex motion has occurred, we can write equation (2.31) as

$$[(I_A/2) + I_B]/\delta I \approx \Omega_c/\delta\Omega_B \ . \tag{2.32}$$

A $Q \gg 1$ event might be initiated by a small-scale crustquake in which $\Delta\Omega_c$ is negative, with this change in Ω_c causing vortex unpinning. The motion of the vortices outward gives rise to a positive shift in Ω_c and may be expected to terminate when the

© American Astronomical Society • Provided by the NASA Astrophysics Data System

1986ApJ...311..197A

net change in Ω_c is zero. Such a sequence of events would be characterized by a sudden change in $\dot{\Omega}_c$ without an accompanying step in Ω_c.

We can write, for a mixed event, the intitial frequency increase followed by the response of the vortex creep torque as

$$\Delta\dot{\Omega}_c(t) = Q^{-1}\Delta\Omega_{c,u}\delta(t) + \Delta\dot{\Omega}_{c,r}(t) , \qquad (2.33)$$

where $\Delta\dot{\Omega}_{c,r}(t)$ is given by equation (2.6). Note that a mixed event has a nonzero mean

$$\lim_{T\to\infty} \int_{0^-}^{T} \Delta\dot{\Omega}_c(t)dt = (Q^{-1} - 1)\Delta\Omega_{c,u} \equiv (1 - Q)\Delta\Omega_c , \qquad (2.34)$$

which would show up as a DC component in the power. The full power spectrum for a process consisting of event with a nonzero mean is given by

$$P_{\dot{\Omega}}(f) = R\,|\,S(\omega)\,|^2 + R^2\,|\,S(0)\,|^2\delta(f) . \qquad (2.35)$$

Thus, the presence of a nonzero mean of the individual events does not affect the power spectrum at finite frequencies. We therefore continue to use equations (2.20) and (2.21) to calculate the power spectrum.

The power spectrum for shot noise consisting of mixed events can be obtained from the results of § II*a* by replacing $\Delta\Omega_{c,u}\delta(t)$ by $\Delta\Omega_c\delta(t)$ and $S(\omega)$ by $S(\omega) + (1 - Q)\Delta\Omega_c$. Hence we have, for $t_0 \ll \tau$,

$$S(\omega) = \Delta\Omega_c[(1 - Q) + i\omega\tau]/(1 + i\omega\tau) , \qquad (2.36)$$

$$P_{\dot{\Omega}}(f) = R(\Delta\Omega_c)^2[(1 - Q)^2 + (\omega\tau)^2]/(1 + \omega^2\tau^2) , \qquad (2.37)$$

and, for $t_0 \gg \tau$, and $\omega t_0 \ll 1$,

$$S(\omega) = [(I_A/6 + I_B/2)\delta\Omega_B\, i\omega t_0 + (Q^{-1} - 1)(I_A/2 + I_B)\delta\Omega_B]/I_c , \qquad (2.38)$$

$$P_{\dot{\Omega}}(f) = R(\Delta\Omega_c)^2(1 - Q)^2 + Q^2[(I_A + 3I_B)/3(I_A + 2I_B)]^2\omega^2{t_0}^2 , \qquad (2.39)$$

while for $t_0 \gg \tau$, and $\omega t_0 \gg 1$,

$$S(\omega) = \Delta\Omega_{c,u} + (1 - Q)\Delta\Omega_c = \Delta\Omega_c , \qquad (2.40)$$

$$P_{\dot{\Omega}}(f) = R(\Delta\Omega_c)^2 . \qquad (2.41)$$

From equations (2.37), 2.39), and (2.41), we note that

$$\lim_{\omega\to 0} P_{\dot{\Omega}}(f) = R(\Delta\Omega_c)^2(1 - Q)^2 , \qquad (2.42)$$

$$\lim_{\omega\to \infty} P_{\dot{\Omega}}(f) = R(\Delta\Omega_c)^2 , \qquad (2.43)$$

with the turnover occurring at $\omega \approx 1/\tau$ if $\tau \gg t_0$ or at $\omega \approx 1/t_0$ if $t_0 \gg \tau$. For $(1 - Q)^2 > 1$, the power spectrum has the form given in Figure 3*a*, while for $(1 - Q)^2 < 1$, the power spectrum is that given in Figure 3*b*. The transition from one type of power spectrum to the other occurs at $Q = 2$, at which value the power spectrum is white noise. Note that pairs of values of Q, Q_1 and Q_2, which satisfy the condition

$$(1 - Q_1) = -(1 - Q_2) \qquad (2.44)$$

will yield the same power spectrum. Thus it suffices to consider $-\infty \leq Q \leq 1$ to represent all formal possibilities, $-\infty < Q < \infty$. The interval $1 \leq Q \leq 2$ is represented by $0 < Q < 1$, and $2 \leq Q \leq \infty$ by $-\infty \leq Q \leq 0$.

We further note that the spectrum given by equation (2.37) for the case $t_0 \ll \tau$ has the same mathematical form as the power spectrum obtained for the two-component model (Deeter 1981). However, in the two-component model of Baym *et al.* (1969), the physical meaning of Q as a fractional inertial moment restricts its values to the range $0 \leq Q \leq 1$; in the present description, all values of Q are possible.

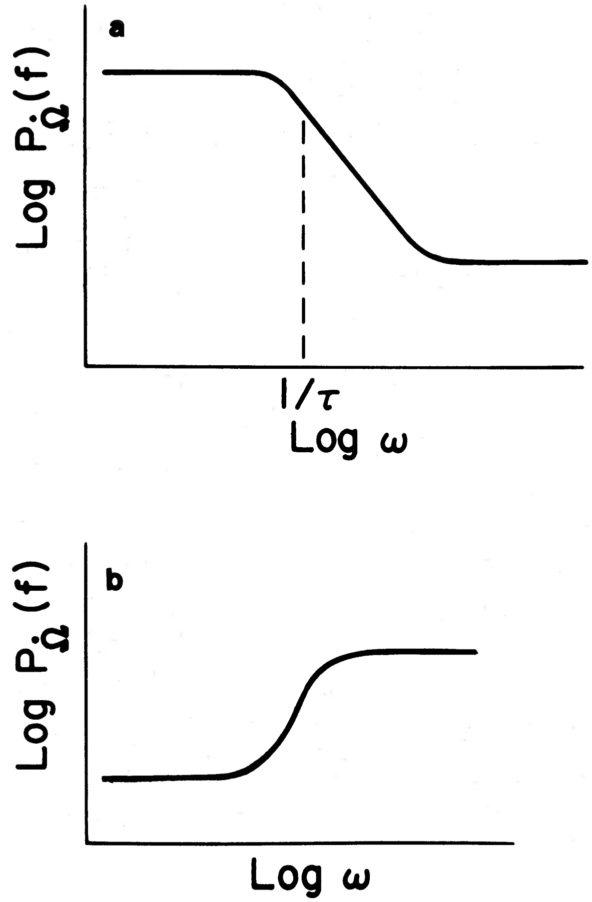

FIG. 3.—Logarithmic of power density for noise resulting from mixed events, (*a*) when $(1 - Q^2) > 1$ and (*b*) when $(1 - Q^2) < 1$.

For large ω (short time scales), only the initial portion $\Delta\Omega_c\delta(t)$ is sampled from each event, and the spectrum appears white. Unlike the pure unpinning events, for mixed events, the behavior in the limit $\omega \to 0$ depends on Q, since at the corresponding long time scales, both the initial event and the response are sampled, and the power spectrum reflects the scaling between the initial event and the response. In this limit we have $P_{\dot{\Omega}}(Q) = R(\Delta\Omega_c)^2(1 - Q)^2$. The power spectrum at intermediate frequencies also depends on Q. For $(1 - Q)^2 \gg 1$, the power density must decrease from $\omega \to 0$. There will be an intermediate range of frequencies (time scales) such that $1 \ll \omega\tau \ll |\,1 - Q\,|$. Since $|\,Q\,| \gg 1$, the initial event $\Delta\Omega_c$ is nebligible in comparison to the response $\Delta\Omega_{c,u}$, while $1 \ll \omega\tau$ means that this response is not sampled to relaxation. Thus the events are like step functions, and the power spectrum indeed has the random walk signature $P_{\dot{\Omega}}(f) \propto \omega^{-2}$. The full spectrum for $|\,1 - Q\,| \gg 1$ is sketched in Figure 3*a*. In the opposite range of Q values, $(1 - Q)^2 \ll 1$, we approach the pure unpinning case, and $P_{\dot{\Omega}}(f) \propto \omega^2$ behavior obtains in the range of frequencies (time scales) $(1 - Q)^2 \ll \omega\tau \ll 1$, as was discussed above (see Fig. 3*b*).

© American Astronomical Society • Provided by the NASA Astrophysics Data System

c) Events Without Vortex Unpinning

If we consider sudden jumps in Ω_c which do not involve vortex motion, the only contribution of the pinned superfluid to the noise is the response of the vortex creep torques. In this case initially $\delta\omega \equiv \Delta\Omega_c$ everywhere in the pinned superfluid and $\Delta\dot{\Omega}_{c,r}(t)$ is given by

$$\Delta\dot{\Omega}_{c,r}(t) = -\frac{I_p|\dot{\Omega}_\infty|}{I_c}\frac{[(e^{t_0/\tau}-1)e^{-t/\tau}]\theta(t)}{1+(e^{t_0/\tau}-1)e^{-t/\tau}}, \quad (2.45)$$

where $t_0 = \Delta\Omega_c/|\dot{\Omega}_\infty|$. The Q for this process is given by

$$Q = I_p/I_c, \quad (2.46)$$

as one might expect for the response of the pinned superfluid to events external to the pinned superfluid. Since $I_p/I_c \approx 10^{-2}$, the response is of negligible magnitude compared to the initial event. From equation (2.45) we obtain the power spectrum for the case $t_0 \ll \tau$,

$$S(\omega) = [1 - (I_p/I_c)(1/1 + i\omega\tau)]\Delta\Omega_c, \quad (2.47)$$

$$P_{\dot{\Omega}}(f) = R(\Delta\Omega_c)^2[(1 - I_p/I_c)^2 + \omega^2\tau^2]/(1 + \omega^2\tau^2). \quad (2.48)$$

For the case $t_0 \gg \tau$, the spectra are, again, somewhat more complicated. However, in all cases, one obtains essentially white noise spectra. As equation (2.48) shows, the deviation from white noise is only of the order of (I_p/I_c) at $\omega \approx \tau^{-1}$ or $(t_0{}^{-1})$. Since $(I_p/I_c) \approx 10^{-2}$, deviations from white noise will not be observable. Note that here we have discussed a model where the power spectrum of the initial events is white noise. In general, for an arbitrary power spectrum of the initial events, the vortex creep response will introduce a deviation of order $(2I_p/2I_c)$ only from that power spectrum.

III. COMPARISON WITH OBSERVATIONS

Boynton and Deeter (1985) have analyzed the noise power spectra of 23 pulsars in addition to the Crab and Vela pulsars. In computing the power spectra of these pulsars from their phase data, they have applied the power estimator techniques of Deeter and Boynton (1982) and Deeter (1984). They have applied clubic and quartic estimators to the phase residual data on a hierarchy of time scales descending by octaves from the entire length of the data span. Applying a cubic (quartic) estimator is equivalent to removing a quadratic (cubic) polynomial from the observed phase data. In the Vela pulsar a large secular cubic term has been observed both in its postglitch relaxation data (Downs 1981) and in the noise spectrum analysis based on power estimator techniques (Boynton and Deeter 1984). The advantage of using quartic estimators is that the resulting noise power spectra are free from contamination by a secular cubic term. The power estimate at any given time scale is based on a large number of degrees of freedom, and the calculation of the power spectrum with one-octave frequency resolution allows one to examine theoretical models with this representation.

The power spectra that have been constructed for pulsars span a frequency range of 2×10^{-4} to 1.6×10^{-2} day^{-1}. The low-frequency limit is determined by the total length of the data span. The high-frequency limit is due to the counting statistics of the finite number of photons detected, as well as contributions from physical processes that lead to changes in pulse shape; both effects lead to white noise in the phase estimates. Pulse shape noise which is white in phase shows up as ω^4 noise when the noise power is described in terms of the angular acceleration $\dot{\Omega}$. The fluctuations introduced into the phase estimates from intrinsic noise dominates this white phase noise at low frequencies, while at high frequencies the opposite is true. The crossover frequency is the frequency at which both contributions are the same. At frequencies higher than the crossover frequency, the intrinsic noise becomes undetectable (Boynton and Deeter 1979). This is indicated schematically in Figure 4. Boynton and Deeter (1985) have emphasized this by indicating the expected contribution of white phase noise to power estimates when they plot the actual power spectra. For each pulsar, they have presented the noise power density spectrum as the logarithm of power in the acceleration $\dot{\Omega}$ as a function of logarithm of frequency.

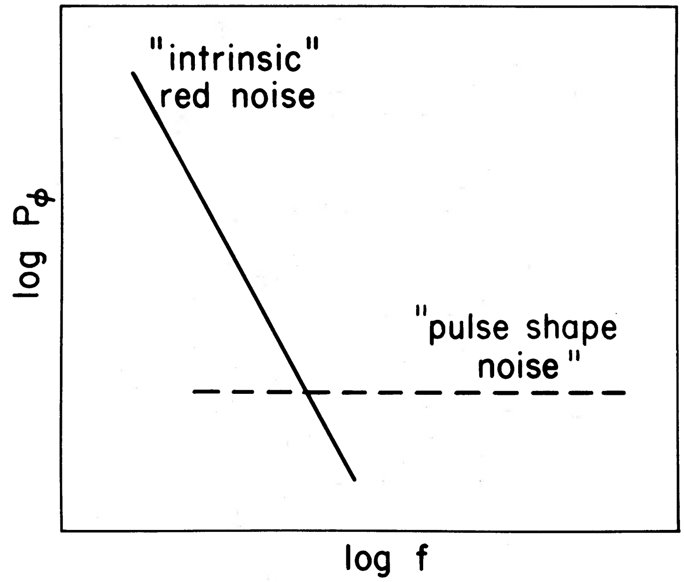

FIG. 4.—Limitation on observability of intrinsic red phase noise dominated by pulse phase measurement uncertainty (from Deeter 1981).

The observed power at any given frequency may be written as the sum of the observational noise and an intrinsic noise contribution,

$$P_{\dot{\Omega}}(f) = P_{\rm in}(f) + P_{\rm obs}(f). \quad (3.1)$$

Boynton and Deeter (1985) have fitted a pure power-law spectrum of the form $P_{\rm in}(f) = cf^b$ to all the pulsars; they find a wide range of exponents. If there are candidates that exhibit a pure power-law spectrum with a slope of $+2$, 0, or -2, we can compare our theoretical models with these fits, because these are the piecewise power-law exponents that can be accomodated in the context of our models (cf. eqs. [2.26], [2.37], and [2.48]).

Relaxation processes in the regions responsible for noise will give rise to structure in the observed power spectra. From the power estimates at available frequencies, we can search for the presence of features in the power spectra which would provide information on relaxation time scales. One can then test for the presence of postglitch relaxation time scales in the noise power spectra. Their presence would clearly indicate if glitch and noise processes originate from the same regions of the star.

We have compared our theoretical models with $t_0 \ll \tau$ with the quartic estimator analysis by Boynton and Deeter (1985) of these 25 pulsars. There are several reasons for restricting the comparison to theoretical models with $t_0 \ll \tau$ (eqs. [2.26],

© American Astronomical Society • Provided by the NASA Astrophysics Data System

1986ApJ...311..197A

1986ApJ...311..197A

[2.37], and [2.48]). These models are described by simple expressions involving two parameters, Q and τ, up to a normalization that reflects the noise strength. Though obtained after a substantial effort in observation and data analysis, the power spectra do not permit one to make meaningful three-parameter fits (Q, τ, and t_0) to cover the general case. Furthermore, in the former case, we have an interesting hypothesis to test regarding the values of τ, namely, we can search for the postglitch relaxation times in noise data to see if the data are consistent with noise originating from the same regions of the star that characterize postglitch relaxation. In contrast to this, we have no handle on typical values of t_0 (event sizes); we do not even have any evidence that single narrow range of t_0 values can be expected. The other side of the coin is that in those cases where the data do not reject a $t_0 \ll \tau$ model with a certain τ, that is with a shoulder at $\omega \approx \tau^{-1}$, an alternative model with $t_0' \gg \tau'$ such that $t_0' \approx \tau$ of the first model will be comparable with the present data. Although the models with $t_0 \gg \tau$ are more complicated mathematically, qualitatively they are similar to the $t_0 \ll \tau$ models. We work with the $t_0 \ll \tau$ models, but this ambiguity should be kept in mind in interpreting our results.

Our approach is in the same spirit as that of Boynton's (1981) work on the Crab pulsar. We quantify the range of theoretical parameters that are consistent with the data, by means of a hypothesis test (Lampton, Margon, and Bowyer 1976) similar to the procedure used by Boynton (1981) in his analysis of the noise power spectra of the Crab pulsar and Her X-1. We examine the extent to which the observational data in the form of equation (3.1) may be fitted with a given theoretical model, for various values of the parameters Q and τ; we treat the noise strength $R(\Delta\Omega_c)^2$ as a free parameter. The sum of the squared residuals for each fit is a measure of the accessibility of the chosen parameters in terms of χ^2 test. We express the χ^2 at a given point in terms of a percentage probability with which the parameters are rejected. We then plot these rejection contours of the observed power spectra in the Q^{-1} versus log τ plane.

In considering the observed power spectra, we first note that for pulsars which are relatively quiet, i.e., which display little power in excess of the white phase noise, significant acceptance or rejection confidence contours cannot be obtained. Examples are the pulsars PSR 0031−37, PSR 0628−28, PSR 1604−00, and PSR 2111+46. As a representative of this class, the observed power spectrum of PSR 0031−07 is shown in Figure 5.

Next we note that there are some pulsars which show excess power only at low frequencies and are limited by white phase noise at higher frequencies. In the case of the five pulsars PSR 0355+54, PSR 0950+08, PSR 1237+25, PSR 1818−04, and PSR 2217+47, the fit to theory will depend on the three lowest frequency points, and hence the parameter estimates will not be very reliable. As a representative of this class, the power spectrum of PSR 0950+08 is shown in Figure 6.

We next consider those pulsars in which glitches have been observed and for which the detailed postglitch observations have been fitted with the vortex creep model; the Crab and Vela pulsars, and PSR 0525+21. Their observed noise power spectra are shown in Figures 7–9. The Crab power spectrum is consistent with white noise in $\dot{\Omega}$ over the whole frequency range of observation, while that of the Vela pulsar is significantly red and that of PSR 0525+21 is rather blue. In the case of the Crab pulsar, very small values of τ, say $\tau < 1$ day, and a value of $Q \approx 2$ (or, equivalently, $Q \approx 0$) are not significantly rejected by the data with greater than 30% confidence. However, in the case of the Vela pulsar, values of τ in the range of 1–10^4 days are rejected with more than 98% confidence for all values of the parameter Q. In the case of PSR 0525+21, the observed relaxation time, $\tau \approx 150$ days, is not rejected with greater than 60% confidence. The probability of rejection of given values of Q and τ for the Crab pulsar and PSR 0525+21 is shown in Figures 10 and 11 respectively.

We may interpret these results in terms of the three possibilities discussed in § II. We conclude that pure unpinning events are not responsible for the observed noise power spectra in the Crab and Vela pulsars because no structure is observed in the power spectra within the expected range of time scales,

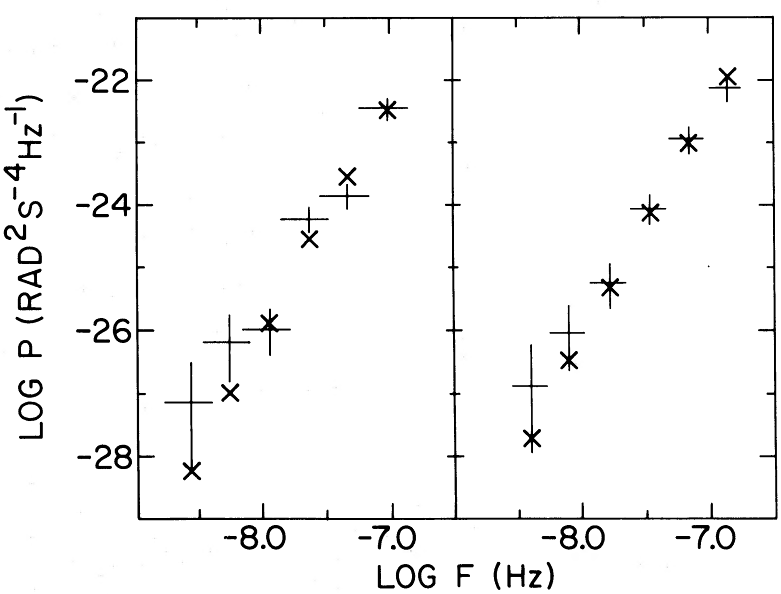

FIG. 5.—Logarithm of power density as a function of logarithm of cyclic frequency for the pulsar PSR 0031−07. The left and right halves of the figure represent the noise power obtained using cubic and quartic estimators respectively. Note: There is hardly any excess power above pulse shape noise.

© American Astronomical Society • Provided by the NASA Astrophysics Data System

1986ApJ...311..197A

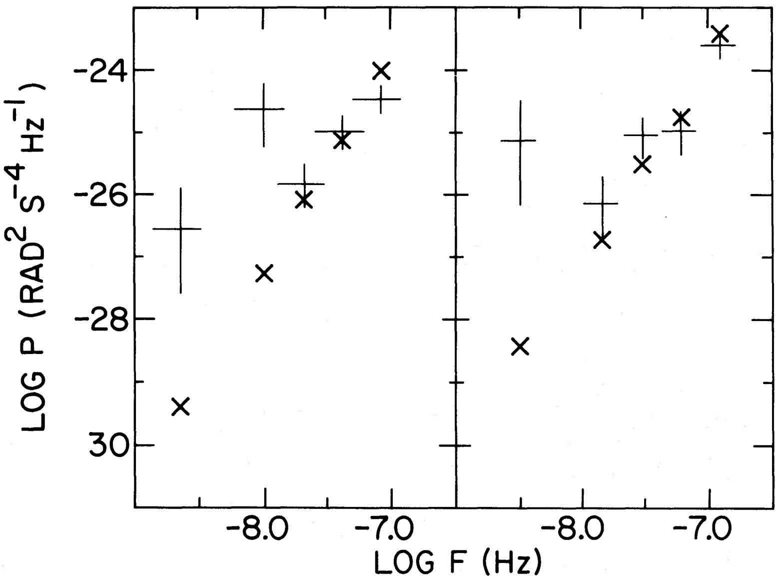

FIG. 6.—Logarithm of power density vs. logarithm of cyclic frequency for the pulsar PSR 0950+08. Note: There is excess power above pulse shape noise only at low frequencies.

$3 \lesssim \tau \lesssim 60$ days for $Q = 1$. It follows that there is not a continuous range of sizes of unpinning events from the glitches all the way down to unresolved events that lead to noise. In other words, in these and possibly other pulsars, in the regions of the star characterized by postglitch relaxation times, there exists a threshold for glitches. Since mixed events ($Q \neq 1$) with a range of relaxation times consistent with those observed in postglitch behavior would also lead to structure which is not observed, hypothesis (2) can also be ruled out, except for $Q \approx 2$ in the case of the Crab pulsar. Note, however, that mixed events with $Q \approx 2$ cannot be distinguished from white noise in the power spectrum. On the other hand, the observations are consistent with hypothesis (3): that the noise is due to physical processes in regions external to the pinning region.

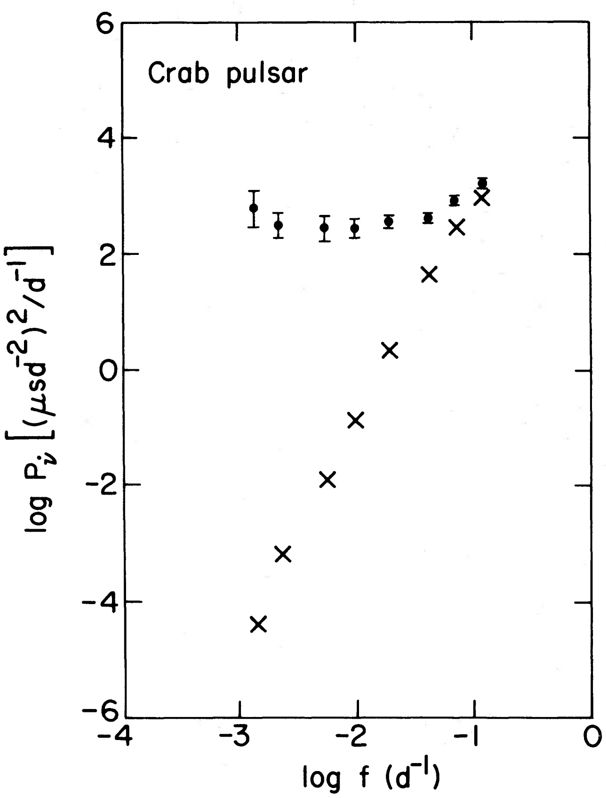

FIG. 7.—Logarithm of power density vs. logarithm of cyclic frequency for the Crab pulsar.

For the Crab pulsar, this conclusion differs from that reached by Boynton (1981). In the two-component model that Boynton was testing, the core superfluid, which constitutes a substantial portion of the star, is assumed to be responding on postglitch time scales to noise originating in the stellar crust, and hence structure at a significant level should be observable on the power spectrum at these time scales. In our present view, the core superfluid is dynamically part of the crust on time scales $\gtrsim$minutes for the Crab and Vela pulsars, so that only the pinned crustal superfluid, with $(I_p/I_c) \approx 10^{-2}$, can participate in the response. Since $I_p \ll I_c$, structure in the timing noise associated with the pinned superfluid response is too weak to be observed.

Finally, we note that in the case of PSR 0525+21, pure unpinning events from a superweak pinning region characterized by a 150 day relaxation time cannot be ruled out at more than a 60% confidence level.

There are 13 pulsars which have reasonable power in excess of pulse shape noise over the entire range of time scales of the observations, so that it is feasible to inquire to what extent the observed noise is consistent with one of the models considered in § II (Boynton and Deeter 1985). We find that in four of these pulsars, PSR 1706−16, PSR 1749−28, PSR 2021+51, and PSR 2045−16, the observed power spectra are quite complicated, in that there appear to be different local power-law exponents at different frequency ranges. Three of the four show a significant excess power at the lowest frequency. Our simple theoretical model is not capable of explaining the structure present in these spectra. For all four, the presence of any thermal creep relaxation time scales from a few days to a few thousand days for any value of the parameter Q is rejected by the data to greater than 90% confidence. In these pulsars, our

© American Astronomical Society • Provided by the NASA Astrophysics Data System

1986ApJ...311..197A

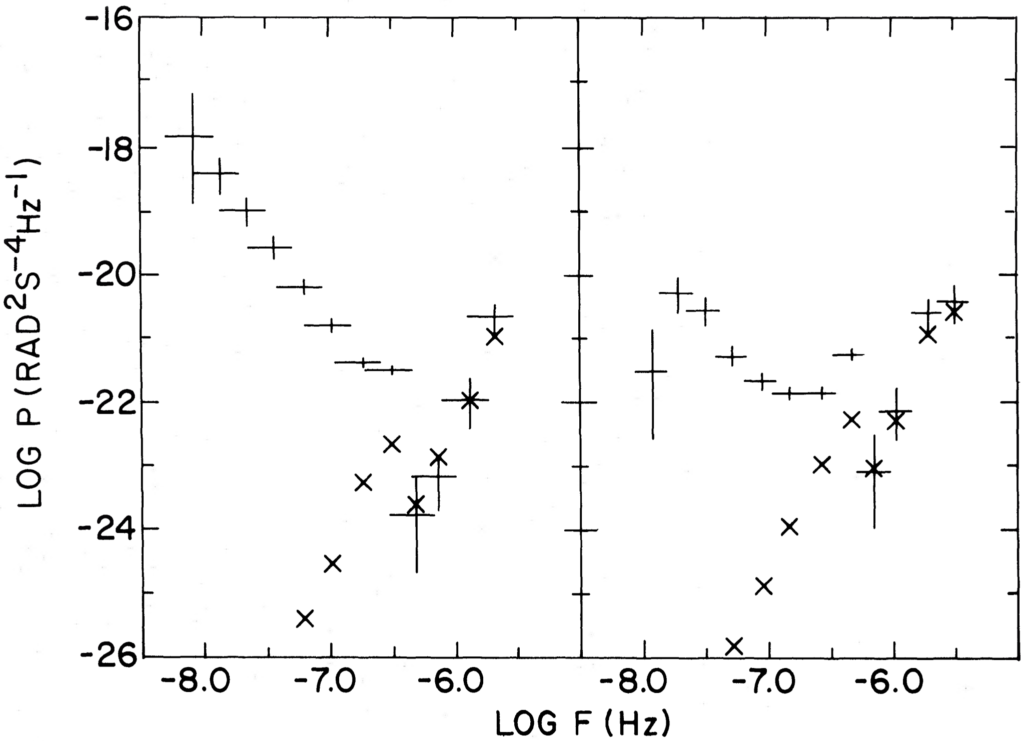

FIG. 8.—Same as Fig. 7, for the Vela pulsar

conclusions are once again that hypotheses (1) and (2) can be ruled out. In the case of hypothesis (3), the response of the pinning region will be unobservable, as indicated above.

To interpret the results of Boynton and Deeter (1985) for the remaining nine pulsars, PSR 0329+54, PSR 0736−40, PSR 0823+26, PSR 1133+16, PSR 1642−03, PSR 1911−04, PSR 1929+10, PSR 1933+16, and PSR 2016+28, we consider a "universal" model for the relaxation times for all old pulsars. Under the hypothesis that the internal structure and the vortex pinning sites in pulsars are the same, the relaxation times in any given pulsar can be expressed in terms of its temperature and the spin-down rate (Alpar, Nandkumar, and Pines 1985). Moreover, making the assumption that heat dissipation due to vortex creep dominates all other processes in older pulsars, the relaxation times that would be observed in the postglitch behavior of such pulsars can be expressed in terms of the spin-down rate alone. Such an assumption has been shown to be consistent with the postglitch behavior of PSR 0525+21. We have calculated the rejection confidence contours in the Q^{-1} versus log τ plane; our results are given in Figures 12–20,

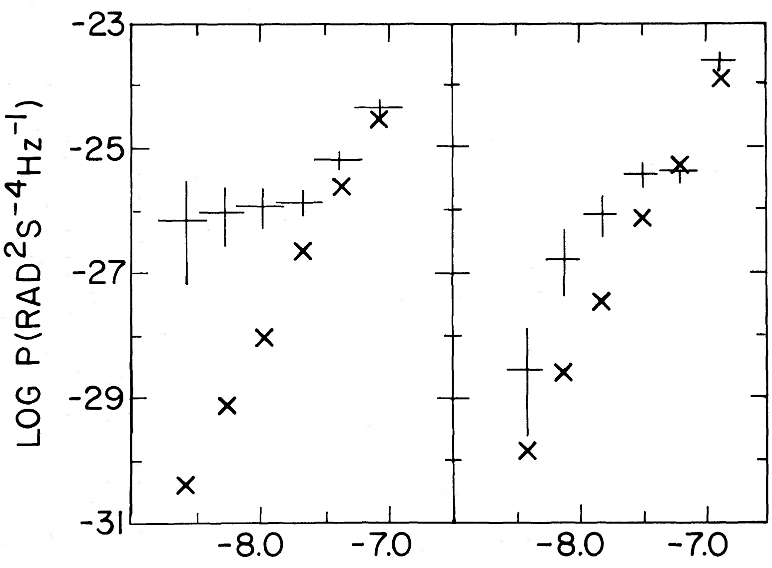

FIG. 9.—Same as Fig. 7, for PSR 0525+21

© American Astronomical Society • Provided by the NASA Astrophysics Data System

1986ApJ...311..197A

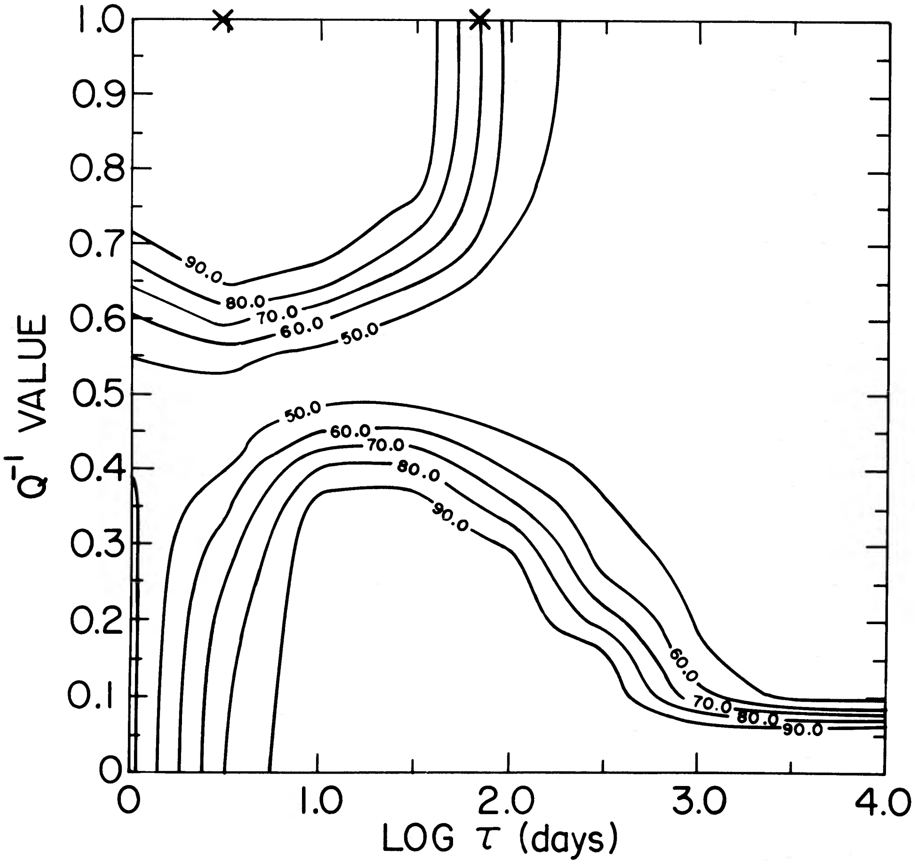

FIG. 10.—Rejection confidence contours in the Q^{-1} vs, log τ plane for the Crab pulsar. Crosses indicate estimated time scales corresponding to superweak and weak regions.

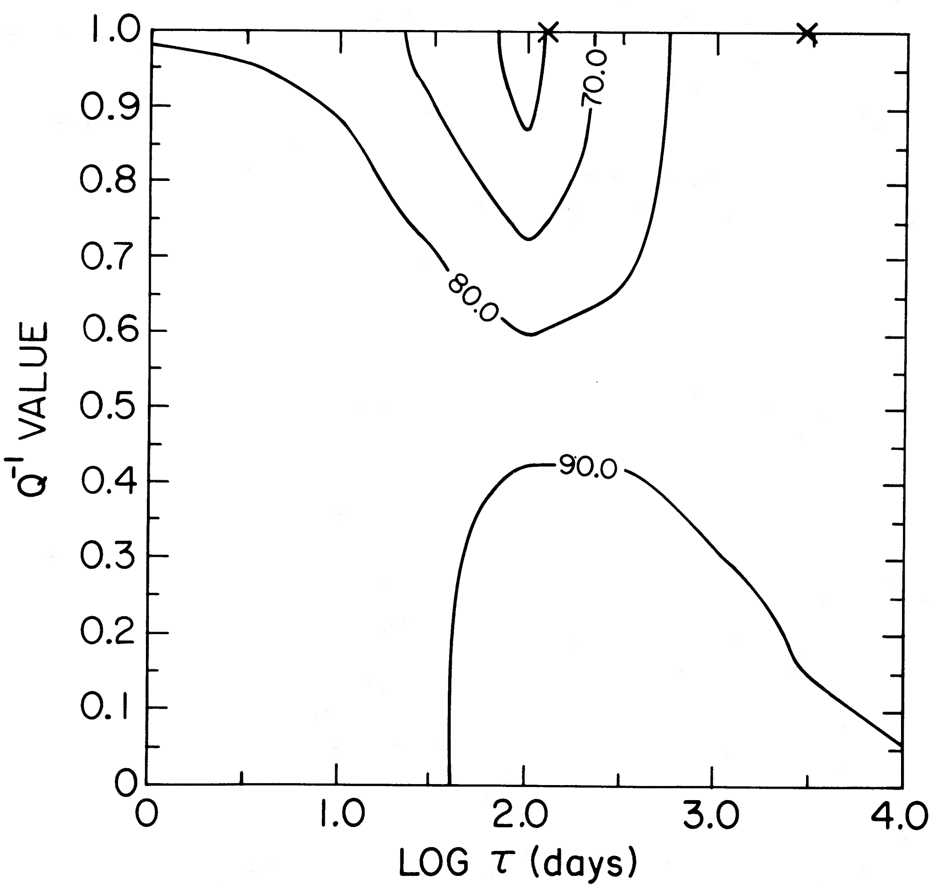

FIG. 11.—Same as Fig. 10, for the pulsar PSR 0525+21

© American Astronomical Society • Provided by the NASA Astrophysics Data System

1986ApJ...311..197A

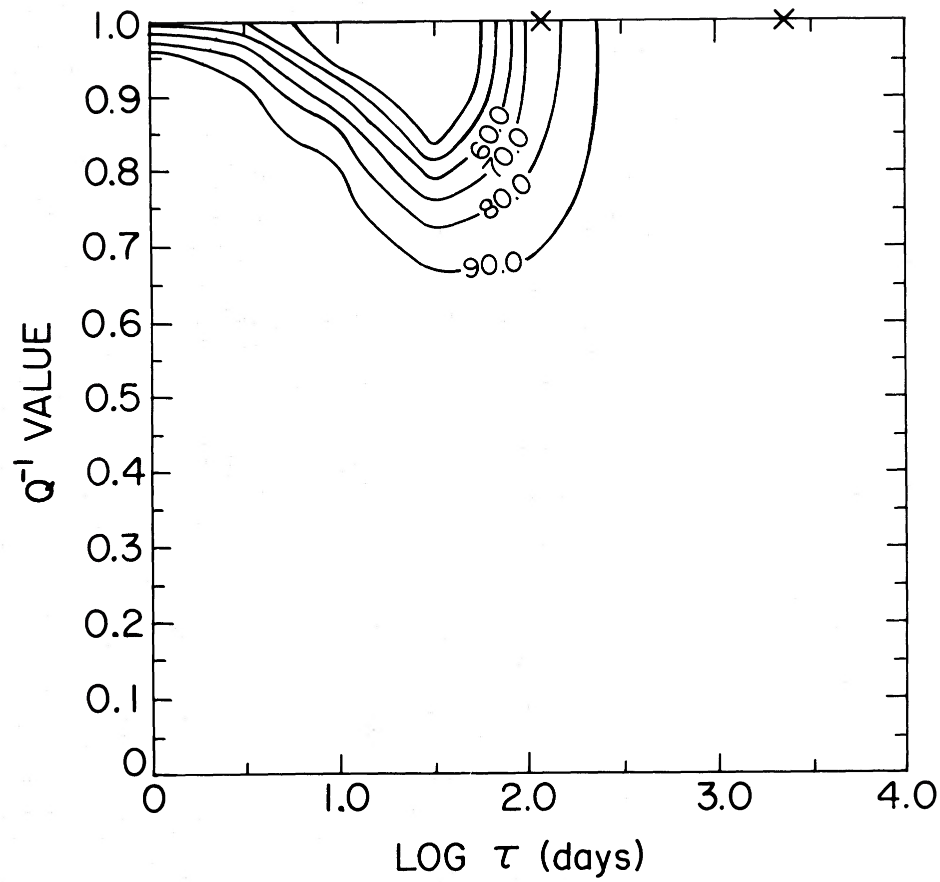

FIG. 12.—Same as Fig. 10, for the pulsar PSR 0329+54

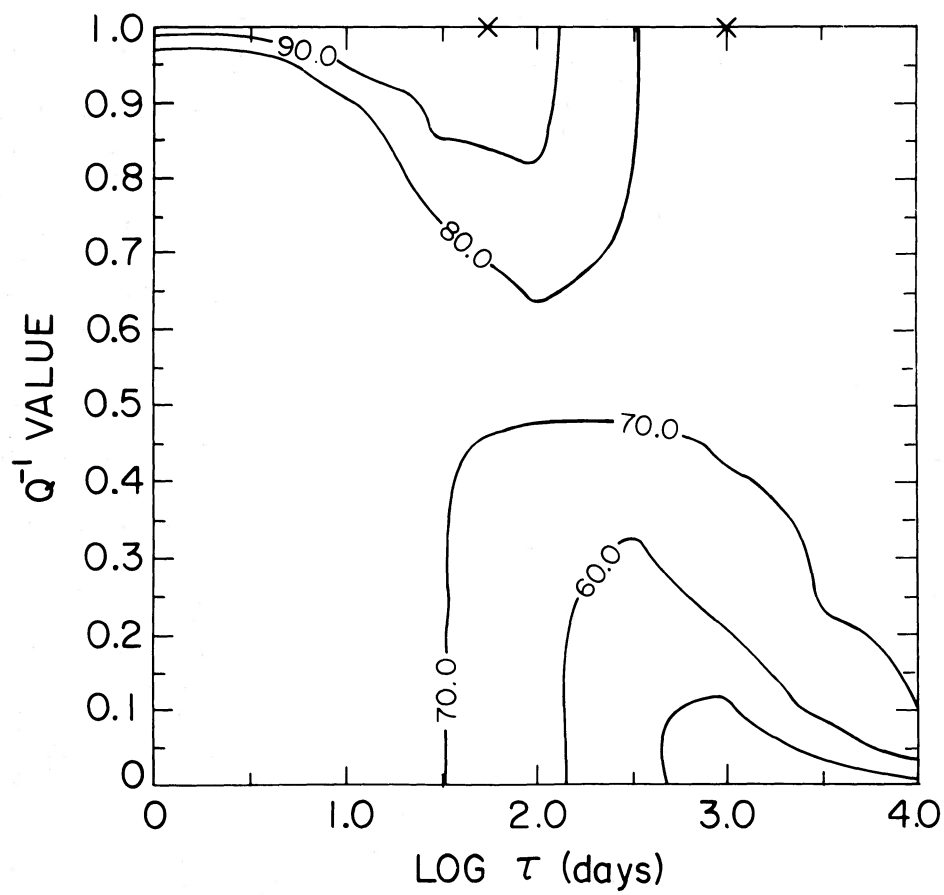

FIG. 13.—Same as Fig. 10, for the pulsar PSR 0736−40

© American Astronomical Society • Provided by the NASA Astrophysics Data System

1986ApJ...311..197A

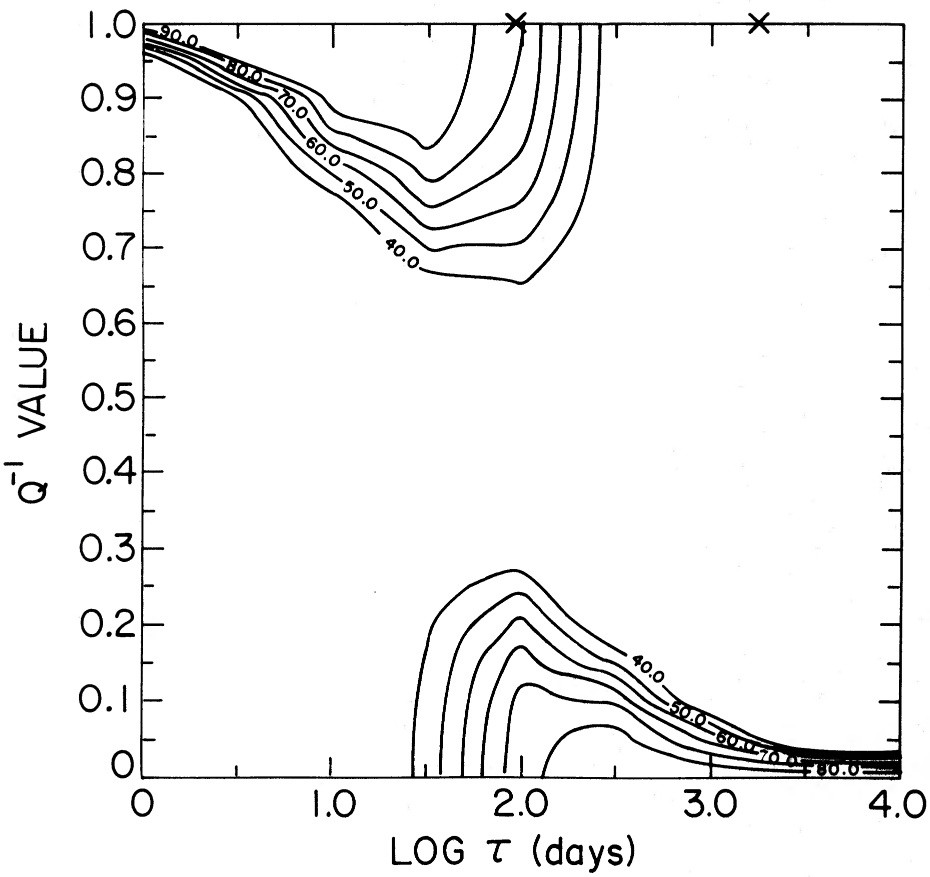

FIG. 14.—Same as Fig. 10, for the pulsar PSR 0823+26

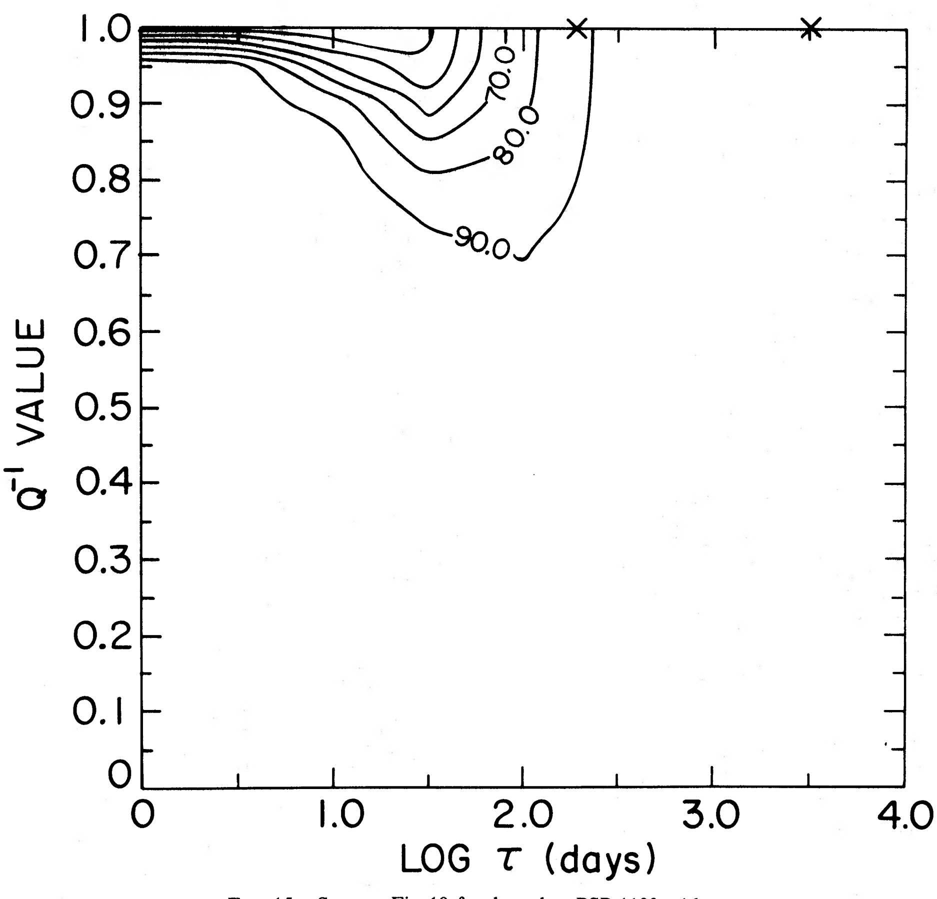

FIG. 15.—Same as Fig. 10, for the pulsar PSR 1133+16

© American Astronomical Society • Provided by the NASA Astrophysics Data System

1986ApJ...311..197A

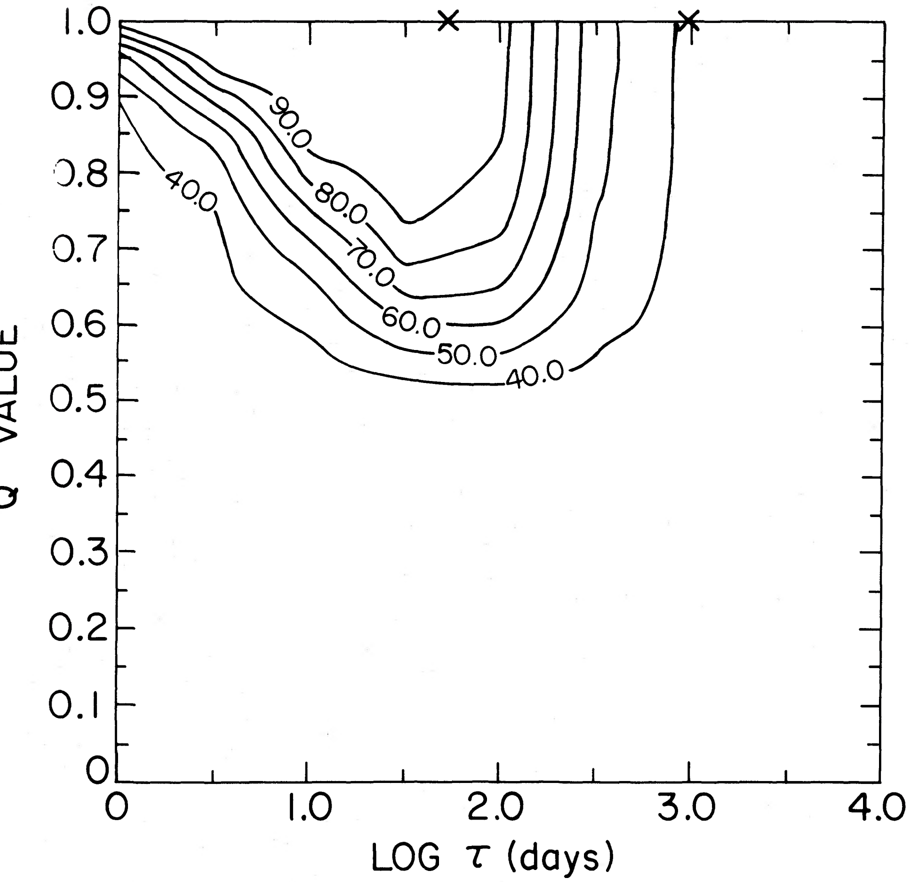

FIG. 16.—Same as Fig. 10, for the pulsar PSR 1642−03

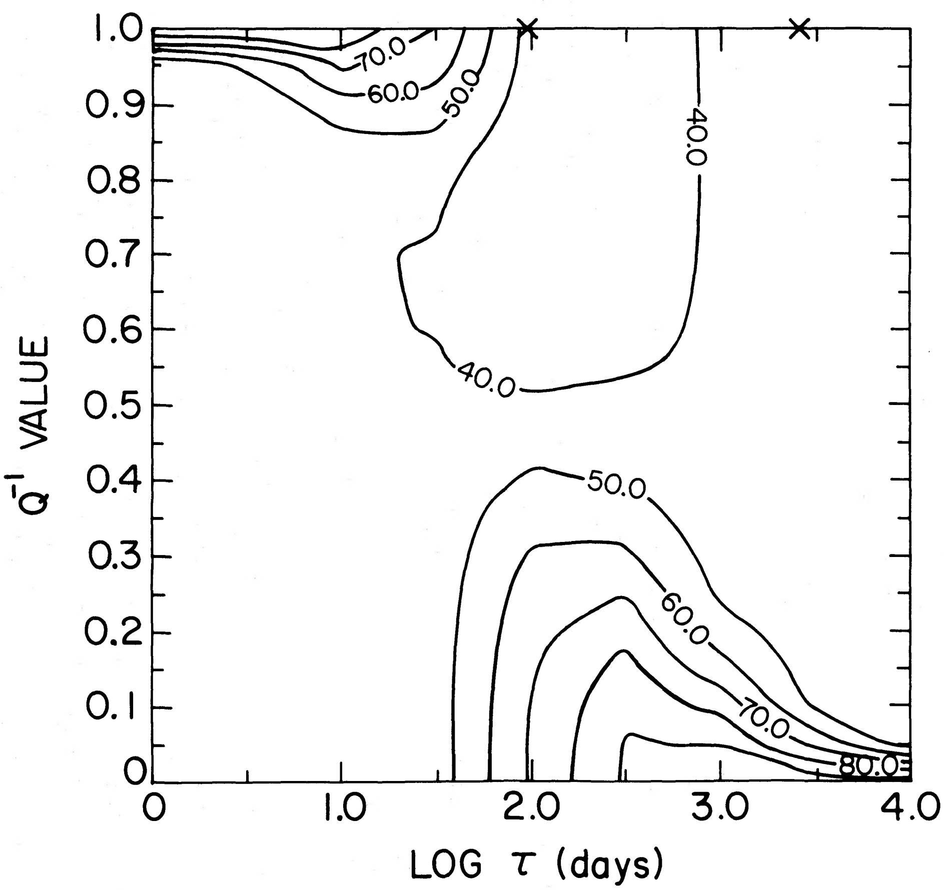

FIG. 17.—Same as Fig. 10, for the pulsar PSR 1911−04

© American Astronomical Society • Provided by the NASA Astrophysics Data System

1986ApJ...311..197A

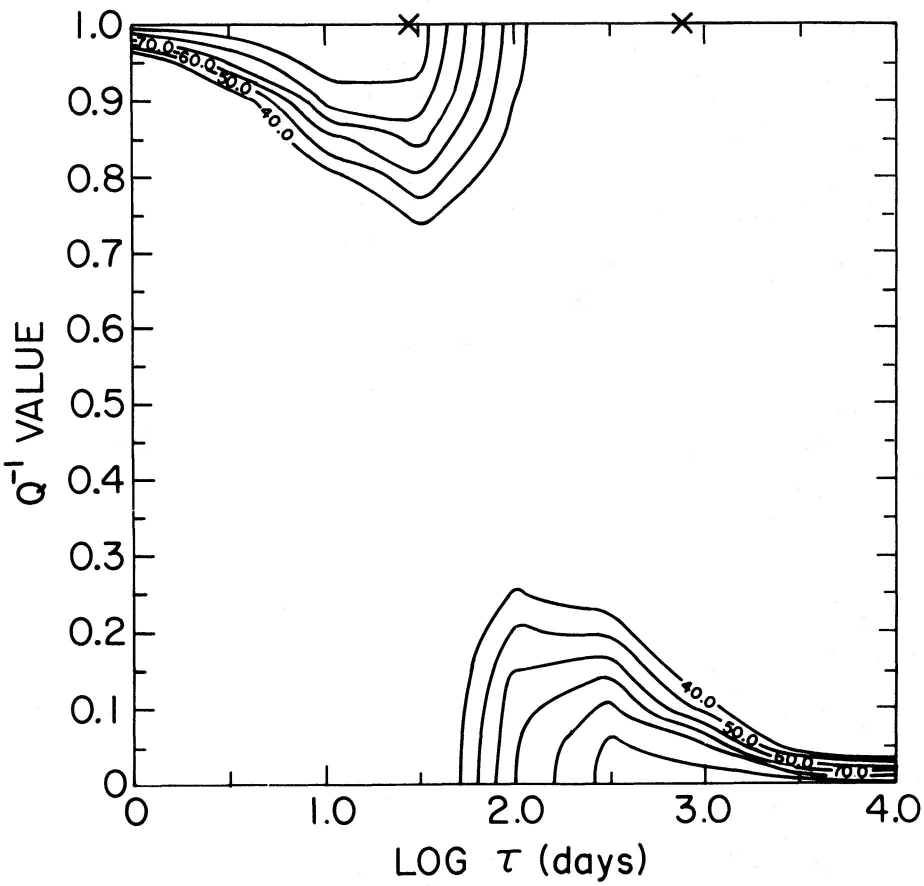

FIG. 18.—Same as Fig. 10, for the pulsar PSR 1929+10

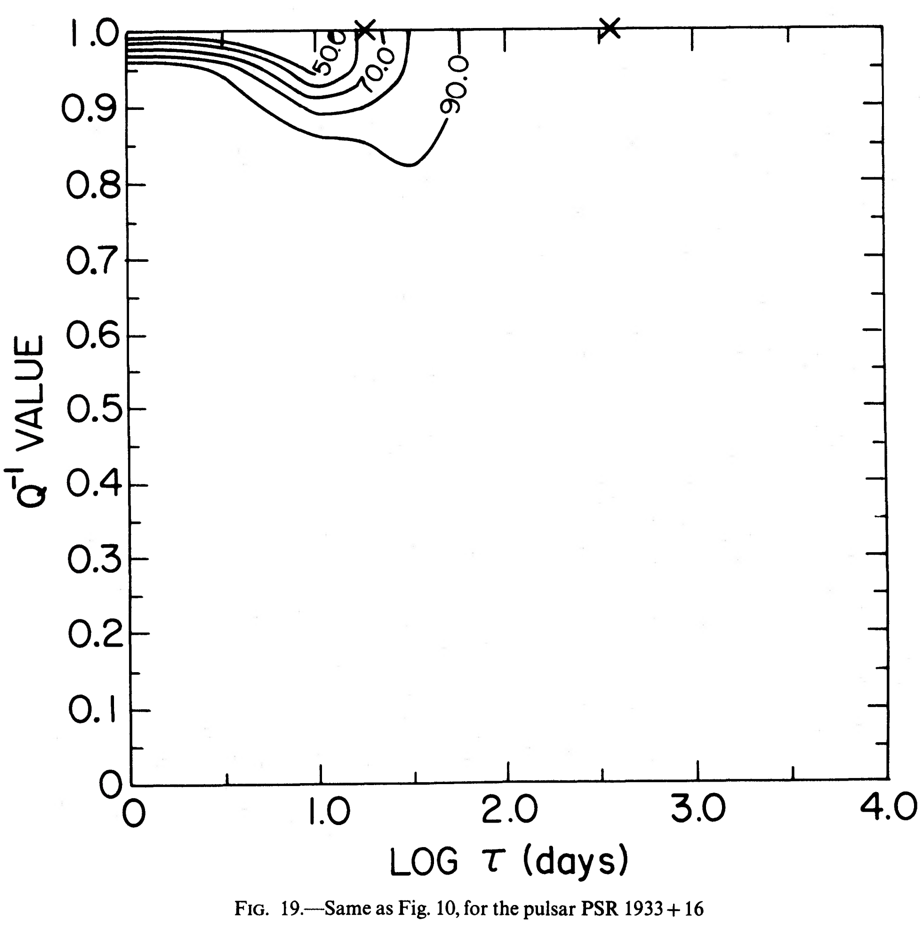

FIG. 19.—Same as Fig. 10, for the pulsar PSR 1933+16

© American Astronomical Society • Provided by the NASA Astrophysics Data System

1986ApJ...311..197A

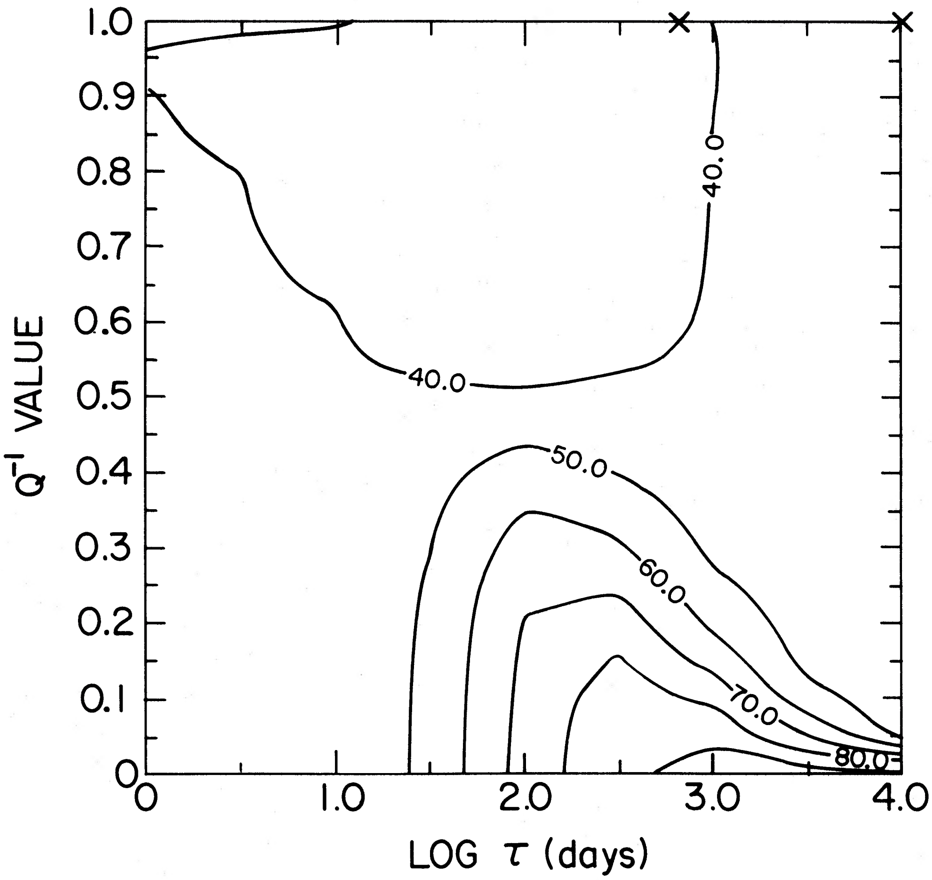

FIG. 20.—Same as Fig. 10, for the pulsar PSR 2016+28

where the crosses indicate the estimated time scales corresponding to superweak and weak regions. We are led to inquire whether, in these pulsars, the regions of the star that are assumed to participate in any postglitch relaxation could make an observable contribution to noise processes.

For three of this last set of nine pulsars, PSR 0329+54, PSR 1133+16, and PSR 1933+16, a rather large range of relaxation time scales is rejected to greater than 90% confidence. This range includes the "extrapolated" relaxation time corresponding to the weak pinning region in all three pulsars. There is a distinct range of parameter space which is not significantly rejected by the data and, for relaxation times within this range, the presence of noise due to pure unpinning, for example, from superweak pinning regions in these stars cannot be ruled out.

For the remaining six pulsars, PSR 0736−40, PSR 0823+26, PSR 1642−03, PSR 1911−04, PSR 1929+10, and PSR 2016+28, the rejection confidence contours show the opposite trend. For pure unpinning events there is a narrow range of relaxation time scales which are significantly rejected with more than 90% confidence; this range includes the relaxation times corresponding to superweak pinning regions in four of these pulsars: PSR 0736−40, PSR 0823+26, PSR 1642−03, and PSR 1929+10. In these pulsars, either hypothesis (1) restricted to the weak pinning regions or hypothesis (2) would be consistent. In the other two pulsars, PSR 1911−04, and PSR 2016+28, none of the three hypotheses can be rejected.

IV. CONCLUDING REMARKS

We have used vortex creep theory to construct model noise power spectra for three physically distinct types of events which might give rise to pulsar timing noise: "pure" events, in which vortex unpinning is the source of the initial frequency jump; "mixed" events, in which the initial frequency jump is produced by some physical process other than vortex unpinning but leads to the unpinning of some vortices; and "external" events, in which the initial frequency jumps responsible for noise do not involve any vortex unpinning. For the first two types of events, we find that relaxation processes in the region responsible for the noise will give rise to structure in the observed power spectra, while for external events, the resulting noise spectra will not be influenced by vortex creep. Hence observation of structure in noise power spectra would not only provide information on the relaxation times which characterize vortex creep but might also provide a clue as to the physical origin of the timing noise.

We have compared our theoretical results with the observed power spectra of Boynton and Deeter (1985) for 25 pulsars. For those pulsars for which observational timing noise is such as to permit a comparison with our theoretical models, we have followed the "standard" Boynton and Deeter procedure of testing for structure in the data associated with various values of Q and τ, while treating the noise strength as a free parameter. This procedure enables us to obtain rejection probability

© American Astronomical Society • Provided by the NASA Astrophysics Data System

1986ApJ...311..197A

contours in the Q^{-1} versus log τ plane. Our comparison of theory with observation for the Boynton-Deeter-JPL sample is given in Table 1. We comment briefly.

For the Crab pulsar, since no structure is observed in the noise power spectrum within the expected ranges of time scales, $3 \lesssim \tau \lesssim 60$ days, we conclude that neither pure nor mixed unpinning events with $t_0 \ll \tau$ can be responsible for the observed timing noise. However, we cannot rule out the presence of these relaxation times in a noise process with $t_0 \gg \tau$, such that the structure at t_0 is beyond the range of observational time scales. For the Vela pulsar, the *shape* of the observed spectrum rules out pure or mixed unpinning processes for $t_0 \gtrsim \tau$ as well as for $t_0 \ll \tau$. Hence for the Vela pulsar, *and possibly for all pulsars*, there exists a threshold for glitches produced by vortex unpinning; put another way, in those parts of the weak and superweak pinning regions which have played a role in postglitch behavior, the energy barriers for vortex creep are such that one does not have a continuous family of glitches, from microglitches associated with the simultaneous unpinning of a comparatively small number of vortex lines to the giant Vela glitches produced by catastrophic unpinning of a very large number of vortex lines. That threshold could be at or near the level of the smallest observed distinct microglitches: $\Delta\Omega/\Omega \lesssim 10^{-10}$. It is possible that PSR 0521+21 shows similar behavior; at present we know only that structure associated with the observed postglitch relaxation time is not rejected with greater than 60% confidence. Recall that where a $t_0 \ll \tau$ spectrum with relaxation time τ is not rejected, a $t_0' \gg \tau'$ spectrum with t_0' in the same range as τ is also viable.

For the remaining pulsars, our searches for structure in the timing data which reflects the relaxation times extracted from our model (see Table 2) has thus far been inconclusive. The absence of observable structure over the time spans searched could, of course, indicate that vortex unpinning plays no observable role in timing noise in these pulsars as well; it is also possible that our extrapolated relaxation times of Table 2 are not valid or that they apply only to postglitch relaxation and not to unpinning noise which originates from regions with

TABLE 1

PRESENT STATUS OF TIMING NOISE OBSERVATIONS AND THEORETICAL CONCLUSIONS BASED ON VORTEX CREEP THEORY

Pulsar	Observational Characteristics of Power Spectra	Theoretical Conclusions
PSR 0031−37, PSR 0628−28, PSR 1604−00, PSR 2111+46	Low noise level; white phase noise dominant at all frequencies	Noise level too small to observe any possible structure
PSR 0355+54, PSR 0950+08, PSR 1237+25, PSR 1818−04, PSR 2217+47	Excess power at low frequencies, white phase noise dominant at high frequencies	Small number of low-frequency data points makes it impossible to draw any meaningful conclusion
PSR 1706−16, PSR 1749−28, PSR 2021+51, PSR 2045−16	Complicated power spectra with different power-law exponents at different frequency ranges	Neither pure nor mixed events can be responsible for observed timing noise
PSR 0531+21 (Crab pulsar)	White noise in $\dot{\Omega}$ over the entire frequency range of observation	Neither pure nor mixed events with the weak or the superweak postglitch relaxation times can be responsible for observed timing noise[a]
PSR 0833−45 (Vela pulsar)	Spectrum significantly red in $\dot{\Omega}$	
PSR 0525−21	Spectrum rather blue in $\dot{\Omega}$	Pure unpinning events from superweak region cannot be rejected with > 60% confidence[b]
PSR 0329+54, PSR 1133+16, PSR 1933+16	No significant structure observed; reasonable amount of power in excess of white phase noise	Broad range of relaxation time scales rejected to $\gtrsim$ 90% confidence level; noise due to pure unpinning ecents in superweak region cannot be ruled out (or in)[b]
PSR 0736−40, PSR 0823+26, PSR 1642−03, PSR 1911−04	Reasonable amount of power in excess of white phase noise; no obvious structure.	Narrow range of relaxation time scales rejected to $\gtrsim$ 9% confidence level; pure unpinning events in weak pinning region or mixed events cannot be ruled out (or in).[b]
PSR 1929+10, PSR 2016+28		Pure or mixed unpinning events in weak or superweak pinning regions cannot be ruled out (or in)[b]

[a] For the Crab pulsar it is possible that postglitch relaxation times are present in unpinning noise, but $t_0 \gg \tau$ and t_0 is outside the observed range of time scales.

[b] Alternatively, the hypothesis that $t_0 \gg \tau$ and t_0 is in the observed range cannot be rejected.

© American Astronomical Society • Provided by the NASA Astrophysics Data System

1986ApJ...311..197A

TABLE 2

OBSERVED Ω, $\dot{\Omega}$ AND PREDICTED RELAXATION TIMES τ FOR THE SUPERWEAK AND WEAK PINNING REGIONS FOR NINE PULSARS

Pulsar	Ω (rad s^{-1})	$\dot{\Omega}$ (10^{-15} rad s^{-2})	τ(sw) (days)	τ(w) (days)
0329+54........	8.79	25.21	111	2220
0736+40........	1.68	72.45	50	1000
0823+26........	11.84	37.45	82	1640
1133+16........	5.29	16.61	151	3020
1642−03........	16.20	74.32	49	980
1911−04........	7.61	37.40	82	1640
1929+20........	27.69	141.50	30	600
1933+16........	17.51	292.60	18	360
2016+28........	11.26	3.03	540	10800

relaxation times τ outside the observed range of time scales. Finally, postglitch relaxation times may also characterize the response to tiny unpinning events but may not show up in the power spectrum if $t_0 \gg \tau$ and t_0 lies outside the range of observed time scales.

A distinct possibility is that physical processes in regions external to the weak and superweak regions so far explored observationally are responsible for the timing noise in all the pulsars studied. If this were the case, then, as we have noted, while vortex creep in the pinning regions could occur in response to individual events, its contribution to the resulting power spectrum would be too small to be distinguishable. The physical origin of the noise could then still be internal (e.g., in the core, in crust-core coupling, or in physical regions in which no appreciable pinning of vortices takes place) or external (in the outer magnetospheric gap, or more generally in the magnetosphere as a whole).

What future observations would be of interest? First of all, it would be desirable to extend the range of the power spectra, to both higher and lower frequencies. The high-frequency end is of special interest, since in this way one could learn whether vortex unpinning events in superweak pinning regions characterized by short ($\lesssim 1$ day)relaxation times are contributing to timing noise. However, such an extension requires frequent (essentially, daily) observations, and data can be obtained in this fashion for only a few comparatively bright pulsars. By extending the low-frequency range, one would be able to search for noise originating in pure unpinning or mixed events in the weak pinning regions characterized by long ($\gtrsim 2000$ days) relaxation times. Second, it would be desirable to expand the number of pulsars in the sample; in so doing, one would obtain better statistics on the absence of features in pulsar noise spectra, as well as acquiring sufficient data to enable one to examine the dependence of noise strength on both the pulsar period and its slowing-down time.

We should like to thank Drs. Paul Boynton, Jim Cordes, John Deeter, and George Downs for sharing their data with us in advance of publication, and for numerous helpful discussions. We should also like to thank our colleagues, F. Lamb, K.-S. Cheng and N. Shibazaki, for helpful discussions on these and related aspects of timing analyses. We are pleased to acknlowledge the support during our research and the preparation of this manuscript provided by the National Science Foundation (grant NSF PHY80-25605), NASA (grant NSG 7653), and NATO (collaborative research grant RG 186.81).

REFERENCES

Alpar, M. A., Anderson, P. W., Pines, D., and Shaham, J. 1984*a*, *Ap. J.*, **276**, 325.
———. 1984*b*, *Ap. J.*, **278**, 791.
Alpar, M. A., Langer, S., and Sauls, J. 1984, *Ap. J.*, **282**, 533.
Alpar, M. A., Nandkumar, R., and Pines, D. 1985, *Ap. J.*, **288**, 191.
Baym, G., Pethick, C. J., Pines, D., and Ruderman, M. 1969, *Nature*, **224**, 872.
Blandford, R., Narayan, R., and Romani, R. W. 1984, *J. Ap. Astr.*, **5**, 369.
Boynton, P. E. 1981, in *IAU Symposium 95, Pulsars*, ed. R. Wielebinski and W. Seiber (Dordrecht: Reidel), p. 279.
Boynton, P. E., and Deeter, J. E. 1979, in *Compact Galactic X-ray Sources, Proc. Washington Workshop*, ed. F. K. Lamb and D. Pines (Urbana: UIUC Physics Dept.), p. 168.
———. 1984, private communication
———. 1985, preprint.
Boynton, P. E., Groth, E. J., Hutchinson, D. P., Nanos, G. P., Partridge, R. B., and Wilkinson, D. T. 1972, *Ap. J.*, **175**, 217.
Cordes, J. M. 1980, *Ap. J.*, **239**, 640.
Cordes, J. M., and Downs, G. S. 1985, *Ap. J. Suppl.*, **59**, 343.
Deeter, J. E. 1981, Ph.D. thesis, University of Washington.
———. 1984, *Ap. J.*, **281**, 482.
Deeter, J. E., and Boynton, P. E. 1982, *Ap. J.*, **261**, 337.
Downs, G. S. 1981, *Ap. J.*, **249**, 687.
Groth, E. J. *Suppl.*, **29**, 453.
Lamb, F. K. 1985, in *Galactic and Extragalactic Compact X-ray Sources*, ed. Y. Tanaka and W. H. G. Lewin (Tokyo: ISAS), p. 19.
Lamb, F. K., Pines, D., and Shaham, J. 1978*a*, *Ap. J.*, **224**, 969.
———. 1978*b*, *Ap. J.*, **225**, 582.
Lampton, M., Margon, B., and Bowyer, S. 1976, *Ap. J.*, **208**, 177.
Rice, S. I. 1954, in *Noise and Stochastic Processes*, ed. N. Wax (New York: Dover), p. 145.
Ruderman, M. 1976, *Ap. J.*, **203**, 213.

M. ALI ALPAR: The Scientific and Technical Research Council of Turkey, Research Institute for Basic Sciences, Tügan-Tbae, P.K. 74 Gebze, Kocaeli, Turkey

RADHA NANDKUMAR: National Center for Supercomputing Applications, University of Illinois, 605 E. Springfield Avenue, Champaign, IL 61820

DAVID PINES: Department of Physics, University of Illinois, 1110 W. Green Street, Urbana, IL 61801-3000

© American Astronomical Society • Provided by the NASA Astrophysics Data System